



Thermal behaviour and kinetics of alga *Polysiphonia elongata* biomass during pyrolysis

Selim Ceylan ^{a,*}, Yıldırıay Topcu ^a, Zeynep Ceylan ^b

^a Ondokuz Mayıs University, Faculty of Engineering, Chemical Engineering Department, 55139 Kurupelit, Samsun, Turkey

^b Ondokuz Mayıs University, Faculty of Engineering, Industrial Engineering Department, 55139 Kurupelit, Samsun, Turkey



HIGHLIGHTS

- This is the first attempt on studying pyrolysis kinetics of *Polysiphonia elongata*.
- Kinetic parameters were determined from TG analysis.
- Pyrolysis process was modeled using obtained kinetic parameters.
- Model was in a good agreement with experimental data.
- Results can be helpful for design of pyrolytic conversion systems.

ARTICLE INFO

Article history:

Received 2 July 2014

Received in revised form 12 August 2014

Accepted 13 August 2014

Available online 22 August 2014

Keywords:

Biomass

Macro algae

Polysiphonia elongata

Pyrolysis

Kinetics

ABSTRACT

The pyrolysis characteristics and kinetics of *Polysiphonia elongata* were investigated using a thermogravimetric analyzer. The main decomposition of samples occurred between 225 °C and 485 °C at heating rates of 5–40 °C/min; owing to release of 78–82% of total volatiles. The heating rate effected pyrolysis characteristics such as maximum devolatilization rate and decomposition temperature. However, total volatile matter yield was not significantly affected by heating rate. The activation energy of pyrolysis reaction was calculated by model free Friedman and Kissenger–Akahira–Sunose methods and mean values were 116.23 kJ/mol and 126.48 kJ/mol, respectively. A variance in the activation energy with the proceeding conversions was observed for the models applied, which shows that the pyrolysis process was composed of multi-step kinetics. The Coats–Redfern method was used to determine pre-exponential factor and reaction order. The obtained parameters were used in simulation of pyrolysis process and results were in a good agreement with experimental data.

© 2014 Elsevier Ltd. All rights reserved.

1. Introduction

Fossil fuels are the main energy sources. However, they are limited and the depletion of these energy sources is expected by the middle of this century (Kraan, 2013). Furthermore, dependence on fossil fuels has largely increased the emissions of greenhouse gases, particulate matters, and other pollutants, which results in many environmental problems such as global warming and atmospheric pollutions. The future supply security of energy sources is another crucial issue. Thus, there has been an increasing interest in alternative and sustainable energy sources. Biomass is one of the most outstanding options as an alternative fuel because it is clean, renewable and fast growing (Kim et al., 2013).

Macro algae have been proposed to have great potential as biomass and they are primarily composed of polysaccharides that can be converted into fuels such as bio-alcohols or bio-oils by fermentation or pyrolysis, respectively (Kim et al., 2012, 2013). This type of biomass is attracting the attention of researchers for its potential as an environmental-friendly and economically sustainable resource. The main advantages include easy of large-scale production, rapid growth, marine environment protective effects. Additionally, their production does not require land or fresh water (Li et al., 2011; Kraan, 2013; Kim et al., 2014a,b).

The pyrolysis is the thermal degradation of materials in the absence of oxygen (Kim et al., 2014a,b) and it is an attractive way to use the energy contained in the biomass. Solid biomass and wastes, which are very difficult and costly to manage, can be readily converted into liquid, gas and charcoal products by the pyrolysis process.

* Corresponding author.

E-mail address: selim.ceylan@omu.edu.tr (S. Ceylan).

Almost all types of biomass can be used as feed stocks for thermochemical conversion. However, thermochemical behavior of various aquatic biomasses is largely different not only from lignocellulosic biomass but also from each other, and the bio-oil produced also varies largely as a result of the differences in components and operation conditions (Kim et al., 2013). Thus, a comprehensive knowledge of the pyrolysis mechanism and kinetic analysis of various marine biomasses is required (Wu et al., 2014).

In addition to this, both the development of the pyrolytic process and reactor design require complete clarification of the pyrolytic mechanism. Therefore, pyrolysis kinetics and thermal decomposition mechanisms for macroalgae should be extensively studied (Li et al., 2011, 2012).

In their recent study, Wang et al. (2013) studied the pyrolysis of macroalgae, *Enteromorpha clathrata* and *Sargassum natans* and compared the composition of biooil products. Yanik et al. (2013) published a study on algal biomass pyrolysis and reported pyrolysis products of *Laminaria digitata* and *Fucus serratus*. Ferrera-Lorenzo et al. (2014a,b) investigated the pyrolysis characteristics of the algae meal which was generated by the industrial production of Agar-Agar. Kim et al. (2012, 2013) investigated the alga *Sagarssum* sp. biomass and *Saccharina japonica* pyrolysis and reported kinetic parameters using reaction models. Wu et al. (2014) studied the pyrolysis of three different aquatic biomass species (microalgae, macroalgae and duckweed) and calculated kinetic parameters by using the thermogravimetric analyzer.

Turkey is surrounded with seas; therefore there is a huge aquatic biomass potential. There is no evidence in literature of the identification of kinetic parameters in the inert atmosphere for *Polysiphonia elongata*. In this work, the pyrolysis behavior and kinetic parameters including apparent activation energy, pre-exponential factor, and reaction order of *P. elongata* (PE), were investigated using TGA. Kinetic constants for the *P. elongata* pyrolysis in the inert atmosphere obtained with different model-free methods were not available in the literature and the results of this study can provide useful knowledge to pyrolysis researchers and engineers. Furthermore, these data are expected to help design and scale up the thermochemical conversion processes for macroalgae *P. elongata*.

2. Methods

2.1. *P. elongata* (PE)

Alga *P. elongata* (PE) was collected from Samsun Harbor, Turkey. The samples were cleaned in fresh water followed by distilled water, dried in oven at 60 °C overnight. The dried samples were pulverized and sieved for 63–125 µm of particle size and used for experiments. PE was characterized in terms of proximate and ultimate analysis, according to the ASTM standards (E871, D1102-84) by using a programmable ash oven. Leco type analyzer CHNS-932 was used for the elemental analysis and oxygen bomb calorimeter was used for the determination of high heating value of PE.

2.2. Thermogravimetric analysis

The TGA of PE was conducted using a Simultaneous Differential Thermogravimetric Analyzer which contains a heat-flux type DTA and a TGA (Shimadzu, DTG-60, Japan; with a precision of temperature measurement ±0.1 K, DTA sensitivity ±0.1 µV and microbalance sensitivity ±0.1 µg). The instrument provided continuous recording of TGA and derivative thermogravimetric (DTG) analysis curves in terms of weight loss percent per second. In each experiment, 10 mg of sample was loaded into the platinum crucible of

the thermal analyzer. To maintain the inert condition, high-purity nitrogen was used as carrier gas. The volume flow rate of nitrogen was 80 mL/min. Non-isothermal experiment runs were carried out at heating rates of 5, 10, 20, and 40 °C/min with temperatures ranging from ambient temperature to 900 °C. All samples were heated to 110 °C and held 20 min (until a constant mass at this temperature was obtained) to provide moisture removal. During heating, sample mass and furnace temperatures were recorded. Each experiment was repeated at least twice for repeatability.

2.3. Kinetic analysis

The kinetics data obtained from TGA are crucial for the efficient design and operation of the pyrolysis process (Liang et al., 2014). As a kind of heterogeneous solid state reaction, general non-isothermal solid decomposition reaction rate can be expressed as in Eq. (1);

$$\frac{dx}{dt} = k(T)f(x) \quad (1)$$

where x is conversion and given by;

$$x = \frac{W_0 - W}{W_0 - W_\infty} \quad (2)$$

In Eq. (2) W_0 , W and W_∞ refer to initial, instantaneous and final weights, respectively. The temperature dependent reaction rate constant $k(T)$ is expressed by Arrhenius equation as;

$$k(T) = A \exp(-E/RT) \quad (3)$$

where A is the pre-exponential factor, E is the activation energy of the reaction, R is the universal gas constant, and T is the absolute temperature.

Substituting Eq. (3) into Eq. (1) gives;

$$\frac{dx}{dt} = Ae^{-\frac{E}{RT}}f(x) \quad (4)$$

where x is conversion; t is reaction time; A is pre-exponential factor; E is activation energy; R is the universal gas constant; T is the absolute temperature. $f(x)$ represents reaction model which is a function of x .

Taking the logarithm of both sides in Eq. (4) yields the Friedman equation, Eq. (5), where the activation energy can be calculated regardless of the decomposition reaction model.

$$\ln\left(\frac{dx}{dt}\right) = \ln A + \ln f(x) - \frac{E}{RT} \quad (5)$$

The activation energy (E) can be obtained from the slope of the curve by plotting $\ln(dx/dt)$ against $1/T$ under a given value of x .

Model free Kissenger–Akahira–Sunose (KAS) method was also applied on the TGA data to obtain E . According to the KAS method, E can be determined from the slope of the lines generated through the linear correlation of $\ln(\beta/T^2)$ with $1/T$ under a given value of x , as shown in Eq. (6) (Gao et al., 2013):

$$\ln\left(\frac{\beta}{T^2}\right) = \ln\left[\frac{AE}{Rf(x)}\right] - \frac{E}{RT} \quad (6)$$

where β shows the heating rate (°C/min).

Model free methods are iso-conversional methods where the activation energy is a function of the conversion (Lopez-Velazquez et al., 2013). These methods are more reliable than model fitting methods in the determination of the activation energy because they can be used without knowledge on the reaction model. In this study, we applied two kinds of model free methods, Friedman and KAS, to obtain the activation energy and kinetic parameters. The intention of choosing those two types of model-free methods was to evaluate and verify the consistency of our

results through two different algorithms: the differential one of Friedman and the integral one of KAS.

The Coats–Redfern method, which has been widely applied to investigate the thermal decomposition was used in this study to obtain the parameters of thermal events. Mean E value from model free methods was used in Coats Redfern equations to determine kinetic parameters, the pre-exponential factor (A) and reaction order (n) (Damartzis et al., 2011; Kantarelis et al., 2011).

The Coats–Redfern equations can be outlined as following (Gao et al., 2013):

Table 1
Proximate and ultimate analysis and higher heating values of PE and some other macroalgae.

	PE	<i>S. japonica</i> ^b	<i>Sargassum</i> sp. ^c
<i>Proximate analysis (%)</i>			
Moisture	11.55	6.90	9.34
Volatile matters	48.20	68.79	44.50
Ash	27.45	20.21	36.82
Fixed carbon	12.80	4.10	9.34
<i>Ultimate analysis</i>			
C	35.81	32.89	26.70
H	5.93	6.17	4.23
N	6.86	0.93	1.35
O	51.40 ^a	60.01	67.53
Higher heating value (MJ/kg)	12.54	12.11	10.10

^a By calculation.

^b Kim et al. (2012).

^c Kim et al. (2013).

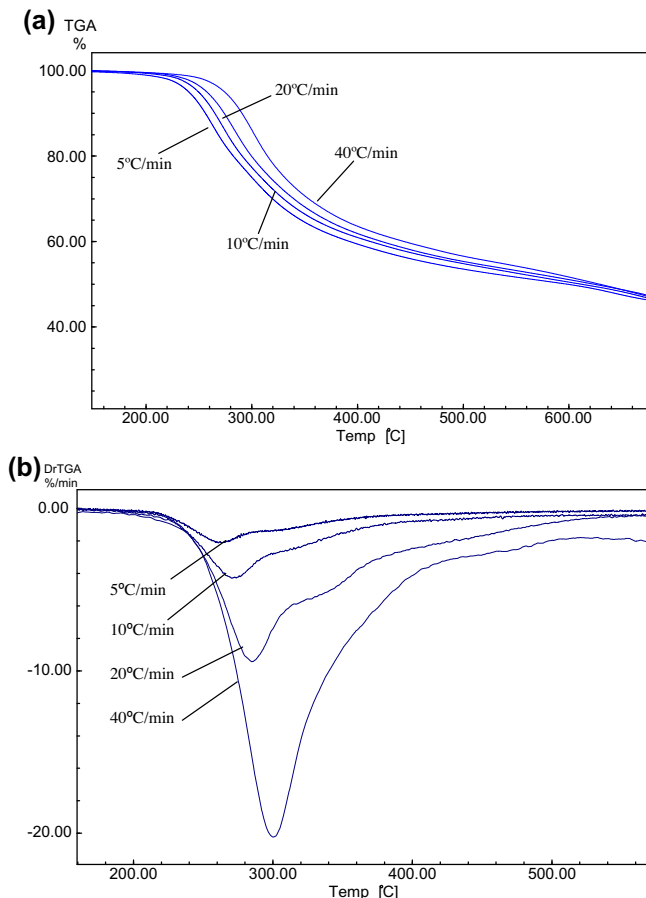


Fig. 1. (a) TGA curves of PE at different heating rates and (b) DTG curves of PE at different heating rates.

$$\ln \left[\frac{1 - (1-x)^{1-n}}{T^2(1-n)} \right] = \ln \left[\frac{AR}{\beta E_a} \right] - \frac{E_a}{RT} \quad (\text{for } n \neq 1) \quad (12)$$

and,

$$\ln \left[\frac{\ln(1-x)}{T^2} \right] = \ln \left[\frac{AR}{\beta E_a} \right] - \frac{E_a}{RT} \quad (\text{for } n = 1) \quad (13)$$

where n , T , A , R , β , and E are the reaction order, absolute temperature, pre-exponential factor, gas constant, heating rate, and activation energy, respectively. In the plot of $\ln \left[\frac{1-(1-x)^{1-n}}{T^2(1-n)} \right]$ versus $\frac{1}{T}$ (for $n \neq 1$) or $\ln \left[\frac{-\ln(1-x)}{T^2} \right]$ versus $\frac{1}{T}$ (for $n = 1$) slope gives $-E/R$. The intercept can be arranged as $\ln \left[\frac{AR}{\beta E_a} \right]$ where A can be calculated (Damartzis et al., 2011).

Table 2
Decomposition characteristics of PE at different heating rates.

Heating rate (°C/min)	T_i (°C)	T_{max} (°C)	T_f (°C)	DTG_{max}	Mass loss ^a (%)
5	226.20	262.26	371.70	0.21	49.72
10	228.12	271.54	402.73	0.41	50.22
20	228.01	284.33	436.46	0.78	50.45
40	227.91	301.54	484.15	1.81	51.03

DTG_{max} – maximum mass loss rate.

T_i – initial decomposition temperature of main decomposition.

T_{max} – temperature at DTG_{max} .

T_f – final decomposition temperature of main decomposition.

^a Mass loss at main degradation stage.

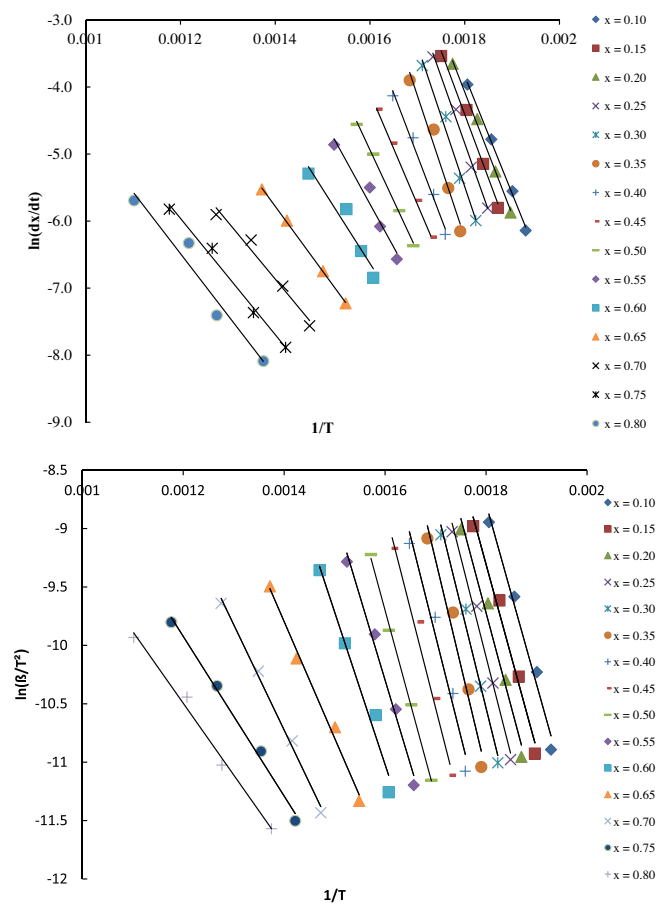


Fig. 2. Plots for determination of activated energy at different conversion by (a) Friedman method and (b) KAS method.

3. Results and discussion

3.1. Characterisation of *P. elongata* (PE)

The results of the proximate analysis, ultimate analysis and higher heating value of PE and the comparison with some macroalgae previously studied can be seen in Table 1. The characteristics of PE were similar with other macroalgae. The volatile matter content of PE was lower than that of *S. japonica* but slightly higher than that of *Sargassum* sp. The ash content was 27.45% for PE and it was between 20.21% and 36.82% for *S. japonica* and *Sargassum* sp., respectively. The low ash content is important because high ash content can cause aggregation in processes and yield inefficient heat transfer rates. It can be seen from results that PE is a carbon and oxygen rich biomass containing 5.93% H and 6.86% N. The empirical formula of PE can be expressed as $\text{CH}_{1.99}\text{O}_{1.08}\text{N}_{0.164}$. The high heating value (HHV) of PE (on dry

biomass) was measured as 12.54 MJ/kg which is slightly higher than that of *S. japonica* and *Sargassum* sp. The higher carbon and hydrogen content can be the reason for the higher value of HHV.

3.2. Thermogravimetric analysis

The mass loss (TG) and differential mass loss (DTG) thermograms of the thermal decomposition of PE, at four heating rates, 5, 10, 20 and 40 °C min⁻¹ under nitrogen atmosphere, are shown in Fig. 1a and b. When the thermogravimetric analysis was conducted, the final weights were 49–51% for each heating rate at 650 °C. Thus, the char content is expected to be approximately 50% indicating the existence of a large amount of inorganic compounds (Kim et al., 2013). The main weight loss occurred in the range of 225–400 °C, with a main peak in the DTG at 280–300 °C and a shoulder approximately between 300–400 °C. Such trends may be attributed to the decomposition of carbohydrates

Table 3

The fitted equations, correlation coefficients (R^2) and activation energies (E , kJ/mol) obtained by the Friedman and KAS methods.

Conversion (x)	Friedman method			KAS method		
	Fitted equation	R^2	E	Fitted equation	R^2	Ea
0.10	$y = -17550x + 27.757$	0.9974	147.57	$y = -15432x + 18.987$	0.9823	128.30
0.15	$y = -18253x + 28.78$	0.9967	151.76	$y = -15799x + 19.132$	0.9856	131.35
0.20	$y = -19025x + 29.835$	0.9901	158.17	$y = -16168x + 19.381$	0.9803	136.91
0.25	$y = -19984x + 31.131$	0.9901	166.15	$y = -16995x + 20.492$	0.9891	141.30
0.30	$y = -21090x + 32.475$	0.9805	175.34	$y = -17490x + 20.946$	0.9841	145.41
0.35	$y = -21204x + 31.92$	0.9747	176.29	$y = -18069x + 21.448$	0.9695	150.23
0.40	$y = -18581x + 26.564$	0.9899	154.48	$y = -17203x + 19.325$	0.9707	143.03
0.45	$y = -16608x + 22.483$	0.9997	138.08	$y = -16935x + 18.255$	0.9809	140.80
0.50	$y = -15144x + 19.291$	0.9966	125.91	$y = -15893x + 15.728$	0.9979	132.13
0.55	$y = -12846x + 14.807$	0.9522	103.81	$y = -14364x + 12.685$	0.9875	119.42
0.60	$y = -11121x + 11.16$	0.9514	92.46	$y = -13071x + 9.8923$	0.9728	108.67
0.65	$y = -10063x + 6.0171$	0.9980	83.66	$y = -9975.5x + 4.1693$	0.9900	82.94
0.70	$y = -9662.1x + 7.7476$	0.9993	80.33	$y = -9030.9x + 1.9184$	0.9949	75.08
0.75	$y = -8667.7x + 4.4408$	0.9894	72.06	$y = -6837.6x - 1.7174$	0.9928	56.85
0.80	$y = -8533.3x + 5.0813$	0.9757	71.11	$y = -6144.1x - 3.1219$	0.9903	51.08

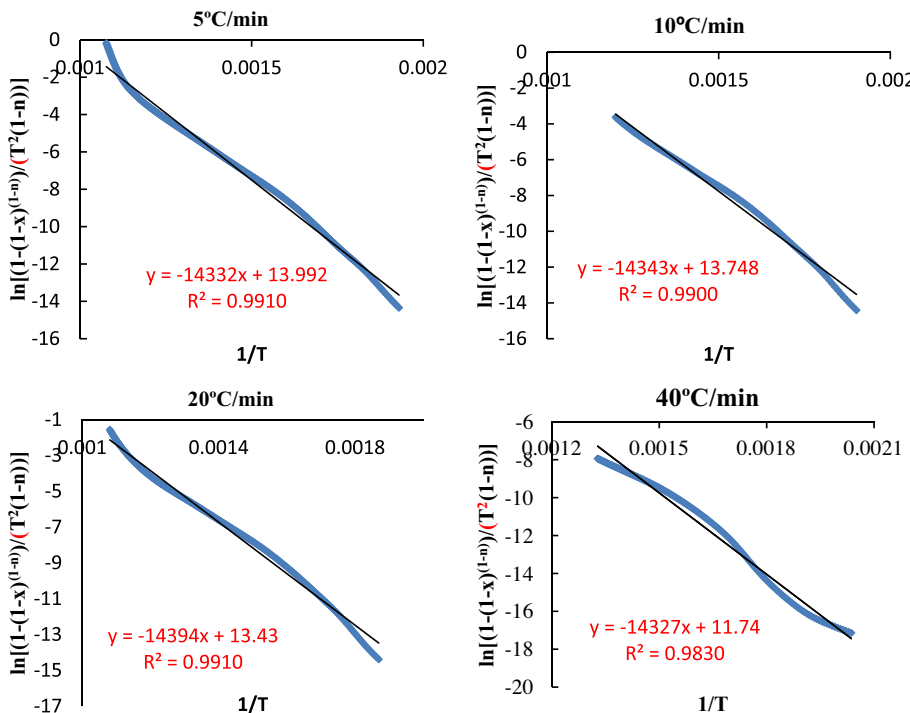


Fig. 3. Coats–Redfern plots for PE at different heating rates.

(225–300 °C) and proteins (300–400 °C) (Bae et al., 2011). Similar results were also observed during the pyrolysis of some other macroalgae (Bae et al., 2011; Kim et al., 2012, 2013; Li et al., 2011). Additionally, as seen in Fig. 1a, above 500 °C a slight weight loss occurred due to further devolatilization of the formed biochar. This phenomenon can be the result of the breakdown of C–C and C–H bonds of the biochar (Liang et al., 2014). As seen in Fig. 1a and b, both TGA and DTG curves showed similar trends for all heating rates. However a slight shift with the increase in heating rate was observed. The heating rate effected the pyrolysis rate and decomposition temperatures during pyrolysis. It also appears that as the heating rate was increased, the thermal degradation process was delayed. At higher heating rates, the samples reach the temperature at a shorter time as the decomposition temperatures were shifted to higher values (Wu et al., 2014). The heating of biomass particles occurs more gradually at lower heating rates, thus enabling an improved and more effective heat transfer to the inner portions and among the particles (Idris et al., 2012; Kim et al., 2013; Gai et al., 2013; Zhao et al., 2013). Therefore, at higher heating rates, the decomposition process proceeded slower due to inefficient heat transfer.

Table 2 represents the decomposition characteristics of PE pyrolysis reaction at different heating rates. As seen in Table 2, the main pyrolysis process proceeds in a range from about 225 °C to 372 °C for low heating rates and 484 °C for high heating rates leading to formation of volatile matter and the biochar. It can be seen both from Table 2 and Fig. 1a and b that the maximum mass loss rate

(DTG_{max}) increases with the increment in the heating rate. When heating rate was 5 °C/min, the DTG_{max} was 0.21 mg/min. However, DTG_{max} increased to 1.81 mg/min when the heating rate was 40 °C/min. The DTG_{max} is a function of the heating rate and increases with the increase in heating rate due to a higher amount of thermal energy which promoted the heat transfer between the surroundings and interiors of the sample (Kim et al., 2013). The peak temperatures were also influenced by the heating rate. As the heating rate increased the maximum peak temperature was slightly shifted to higher temperatures. This can be the cause of heterogeneous structure of macroalgae. At high heating rates, decomposition of carbohydrate and protein components of macroalgae may occur simultaneously. As seen in Fig. 2b, at a heating rate of 40 °C/min, shoulder peak disappeared and an overlapping peak was observed for decomposition of PE (Liang et al., 2014).

3.3. Kinetic analysis

The model free Friedman and KAS methods were used to evaluate the apparent activation energy. Methods were employed at different heating rates ranging from 5 to 40 °C/min, for fractional conversions varying from 0.10 to 0.80 to determine the variation of the apparent activation energy during the thermal decomposition process. The regression lines obtained using Friedman and KAS methods are shown in Fig. 2a and b, respectively. The fitted equations, correlation coefficients (R^2) and activation energies are summarized in Table 3. R^2 values were higher than 0.9700 for all lines. Therefore, it can be concluded from Fig. 2 and Table 3 that the model free methods used are reliable in determining the activation energy. The activation energy, E , based on Eq. (5) can be obtained from a plot of $\ln(dx/dt)$ vs. $1/T$. Fig. 2a presents plots of $\ln(dx/dt)$ vs. $1/T$ at various conversions ranging from 0.10 to 0.80. Similarly, as seen in Fig. 2b, plotting the left side of Eq. (6), $\ln\left(\frac{dx}{dt}\right)$ vs. inverse temperature, $1/T$, for different heating rates, straight lines can be produced. As seen in Fig. 2b, the activation energy can be estimated by the slope of produced straight lines.

Table 4
Kinetic parameters for PE biomass pyrolysis in nitrogen atmosphere.

Heating rate (°C/min)	n	A	R^2
5	7.6	4.88×10^{11}	0.9914
10	8.1	1.07×10^{12}	0.9908
20	8.4	4.47×10^{11}	0.9872
40	7.4	5.00×10^{11}	0.9854

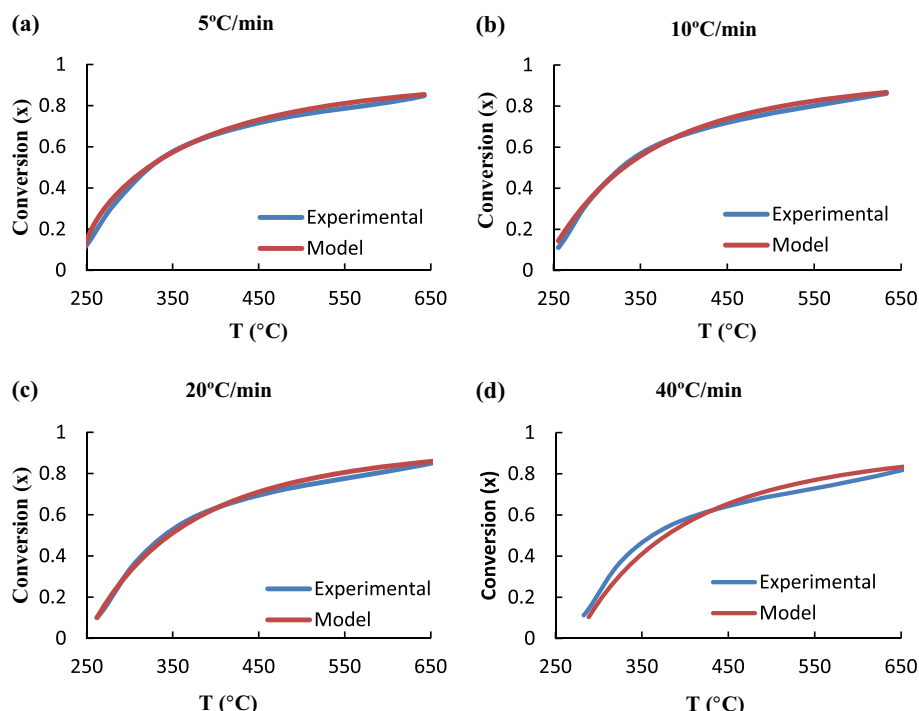


Fig. 4. Simulation of PE pyrolysis using the kinetic data calculated for: (a) 5, (b) 10, (c) 20 and (d) 40 °C/min.

Table 5

Comparision of kinetic parameters obtained from pyrolysis reactions of various marine biomass residues.

Marine biomass	<i>E</i> (kJ/mol)	<i>A</i> (s ⁻¹)	<i>n</i>	Reference
<i>C. vulgaris</i>	332.6	1.3×10^{28}	9.0	Chen et al. (2012)
<i>S. platensis</i>	97.0	9.16×10^7	1.98	Peng et al. (2001)
<i>C. protothecoides</i>	52.5	1.11×10^4	1.88	Peng et al. (2001)
<i>D. tertiolecta</i>	146.067	2.28×10^{13}	2.4	Shuping et al. (2010)
<i>D. tertiolecta</i>	171.85	1.09×10^{14}	5.3	Wu et al. (2014)
<i>E. prolifera</i>	178.89	6.321×10^{10}	5.4	Wu et al. (2014)
<i>P. elongata</i>	121.355 ^a	6.263×10^{11} ^a	7.9 ^a	This study

^a Mean values.

The activation energies calculated by KAS and Friedman methods were slightly different. However, the variations in the activation energy with proceeding conversions were similar in both methods. The activation energy was increased up to 0.35 conversion then it was decreased. The activation energy was increased from 147.57 to 176.29 kJ/mol and decreased to 71.11 kJ/mol in the Friedman method. It increased from 128.30 to 150.23 kJ/mol and then decreased to 51.08 kJ/mol in the KAS method. This trend can be caused by the degradation of carbohydrate and protein content of macroalgae PA (Slopiecka et al., 2012). Mean values were 126.48 kJ/mol and 116.23 kJ/mol for Friedman and KAS methods, respectively. The mean of these values were accepted as the mean activation energy and used in Eqs. (12) and (13) for the calculation of kinetic parameters, including pre-exponential factor and reaction order. As seen from Fig. 3, for all heating rates, *R*² values for Coats–Redfern plots were higher than 0.9800.

The obtained pre-exponential factor and reaction order values at different heating rates are shown in Table 4. It should be noted that these reaction orders which were obtained by iso-conversional methods have no physical meaning and can be considered as fitting parameter (Damartzis et al., 2011; Kantarelis et al., 2011; Liang et al., 2014). The obtained kinetic parameters were used to simulate the pyrolysis process of alga PE. As seen from Fig. 4, model and experimental data were in a good agreement.

A comparison of the kinetic parameters of pyrolysis for PE and some other marine biomasses are shown in Table 5. The activation energy for pyrolysis of PE is similar to the reported values for *D. tertiolecta*, *E. prolifera*. However, the activation energy for *C. vulgaris* was higher. In contrast, the activation energies for *S. plantensis* and *C. protothecoides* were lower than that of PE. An obvious difference also can be seen in the pre-exponential factors and reaction orders. The differences in the kinetic parameters may be due to the differences in the composition of the biomasses. Also, the usage of different experimental conditions and various methods for calculations may cause that the derived kinetic parameters to differ from each other (Slopiecka et al., 2012; Liang et al., 2014).

4. Conclusion

The incorporation of marine biomass, PE, into energy production depends on understanding of the kinetics of pyrolysis and degradation reactions. As a readily available and abundant raw-material, activation energies for PE were comparable to those of previously studied algae residues. A variance in the activation energy with proceeding conversions was observed which revealed that the pyrolysis of PE was composed of multi-step kinetics. This finding was consistent with the reported studies on some other

algae species, *D. tertiolecta*, *E. prolifera*, *S. plantensis* and *C. protothecoides*. A reaction model was established using obtained kinetic parameters and results were in a good agreement with experimental data.

References

- Bae, Y.J., Ryu, C., Jeon, J.-K., Park, J., Suh, D.J., Suh, Y.-W., Chang, D., Park, Y.-K., 2011. The characteristics of bio-oil produced from the pyrolysis of three marine macroalgae. *Bioresour. Technol.* 102, 3512–3520.
- Chen, C., Ma, X., He, Y., 2012. Co-pyrolysis characteristics of microalgae *Chlorella vulgaris* and coal through TGA. *Bioresour. Technol.* 117, 264–273.
- Damartzis, T., Vamvuka, D., Sfakiotakis, S., Zabaniotou, A., 2011. Thermal degradation studies and kinetic modeling of cardoon (*Cynara cardunculus*) pyrolysis using thermogravimetric analysis (TGA). *Bioresour. Technol.* 102, 6230–6238.
- Ferrera-Lorenzo, N., Fuente, E., Bermúdez, J.M., Suárez-Ruiz, I., Ruiz, B., 2014a. Conventional and microwave pyrolysis of a macroalgae waste from the Agar-Agar industry. Prospects for bio-fuel production. *Bioresour. Technol.* 151, 199–206.
- Ferrera-Lorenzo, N., Fuente, E., Suárez-Ruiz, I., Gil, R.R., Ruiz, B., 2014b. Pyrolysis characteristics of a macroalgae solid waste generated by the industrial production of Agar-Agar. *J. Anal. Appl. Pyrol.* 105, 209–216.
- Gai, C., Zhang, Y., Chen, W.-T., Zhang, P., Dong, Y., 2013. Thermogravimetric and kinetic analysis of thermal decomposition characteristics of low-lipid microalgae. *Bioresour. Technol.* 150, 139–148.
- Gao, W., Chen, K., Xiang, Z., Yang, F., Zeng, J., Li, J., Yang, R., Rao, G., Tao, H., 2013. Kinetic study on pyrolysis of tobacco residues from the cigarette industry. *Ind. Crops Prod.* 44, 152–157.
- Idris, S.S., Rahman, N.A., Ismail, K., 2012. Combustion characteristics of Malaysian oil palm biomass, sub-bituminous coal and their respective blends via thermogravimetric analysis (TGA). *Bioresour. Technol.* 123, 581–591.
- Kantarelis, E., Yang, W., Blasiak, W., Fosgren, C., Zabaniotou, A., 2011. Thermochemical treatment of E-waste from small household appliances using highly pre-treated nitrogen-thermogravimetric investigation and pyrolysis kinetics. *Appl. Energy* 88, 922–929.
- Kim, D.-H., Lee, S.-B., Jeong, G.-T., 2014a. Production of reducing sugar from *Enteromorpha intestinalis* by hydrothermal and enzymatic hydrolysis. *Bioresour. Technol.* 161, 348–353.
- Kim, S.W., Koo, B.S., Lee, D.H., 2014b. A comparative study of bio-oils from pyrolysis of microalgae and oil seed waste in a fluidized bed. *Bioresour. Technol.* 162, 96–102.
- Kim, S.-S., Ly, H.V., Choi, G.-H., Kim, J., Woo, H.C., 2012. Pyrolysis characteristics and kinetics of the alga *Saccharina japonica*. *Bioresour. Technol.* 123, 445–451.
- Kim, S.-S., Ly, H.V., Kim, J., Choi, J.H., Woo, H.C., 2013. Thermogravimetric characteristics and pyrolysis kinetics of alga *Sagarssum sp.* biomass. *Bioresour. Technol.* 139, 242–248.
- Kraan, S., 2013. Mass-cultivation of carbohydrate rich macroalge, a possible solution for sustainable biofuel production. *Mitig. Adapt. Strateg. Glob. Change* 18, 27–46.
- Li, D., Chen, L., Chen, S., Zhang, X., Chen, F., Ye, N., 2012. Comparative evaluation of the pyrolytic and kinetic characteristics of a macroalga (*Sargassum thunbergii*) and a freshwater plant (*Potamogeton crispus*). *Fuel* 96, 185–191.
- Li, D., Chen, L., Zhang, X., Ye, N., Xing, F., 2011. Pyrolytic characteristics and kinetic studies of three kinds of red algae. *Biomass Bioenergy* 35, 1765–1772.
- Liang, Y.-G., Cheng, B., Si, Y.-b., Cao, D.-j., Jiang, H.-y., Han, G.-m., Liu, X.-h., 2014. Thermal decomposition kinetics and characteristics of *Spartina alterniflora* via thermogravimetric analysis. *Renew. Energy* 68, 111–117.
- Lopez-Velazquez, M.A., Santes, V., Balmaseda, J., Torres-Garcia, E., 2013. Pyrolysis of orange waste: a thermo-kinetic study. *J. Anal. Appl. Pyrol.* 99, 170–177.
- Peng, W., Wu, Q., Tu, P., Zhao, N., 2001. Pyrolytic characteristics of microalgae as renewable energy source determined by thermogravimetric analysis. *Bioresour. Technol.* 80, 1–7.
- Slopiecka, K., Bartocci, P., Fantozzi, F., 2012. Thermogravimetric analysis and kinetic study of poplar wood pyrolysis. *Appl. Energy* 97, 491–497.
- Wang, S., Wang, Q., Jiang, X., Han, X., Ji, H., 2013. Compositional analysis of bio-oil derived from pyrolysis of seaweed. *Energy Convers. Manage.* 68, 273–280.
- Wu, K., Liu, J., Wu, Y., Chen, Y., Li, Q., Xiao, X., Yang, M., 2014. Pyrolysis characteristics and kinetics of aquatic biomass using thermogravimetric analyzer. *Bioresour. Technol.* 163, 18–25.
- Yanik, J., Stahl, R., Troeger, N., Sinag, A., 2013. Pyrolysis of algal biomass. *J. Anal. Appl. Pyrol.* 103, 134–141.
- Zhao, H., Yan, H., Dong, S., Zhang, Y., Sun, B., Zhang, C., Ai, Y., Chen, B., Liu, Q., Sui, T., Qin, S., 2013. Thermogravimetry study of the pyrolytic characteristics and kinetics of macro-algae *Macrocystis pyrifera* residue. *J. Therm. Anal. Calorim.* 111, 1685–1690.